PHYSICAL REVIEW B VOLUME 17, NUMBER 3 1 FEBRUARY 1978

Raman scattering, superconductivity, and phonon density of states of stoichiometric and nonstoichiometric TiN†

W. Spengler and R. Kaiser
Physik Department der Technischen Universität München, München, Federal Republic of Germany

A. N. Christensen
Department of Chemistry, Aarhus University, Aarhus, Denmark

G. Müller-Vogt
Kristall- und Materiallabor der Fakultät für Physik, Universität Karlsruhe (TH), Karlsruhe, Federal Republic of Germany
(Received 14 September 1977)

Raman scattering and superconductivity of titanium nitride with various N deficiencies have been investigated. While in stoichiometric superconducting TiN second-order Raman scattering is predominant, first-order Raman scattering increases with increasing N deficiency. The first-order Raman spectrum which agrees well with the phonon density of states shifts to higher frequencies when the N deficiency grows. This frequency shift is particularly strong at small N deficiencies ($\sim 5\%$) and is coupled with a drastic drop of T_c. The shift of the phonon density of states indicates phonon anomalies in stoichiometric TiN at 200 cm^{-1} in close agreement with just performed neutron studies. In almost stoichiometric TiN the mean-square frequencies $\langle \omega^2 \rangle$ from the Raman spectra are in good agreement with corresponding specific-heat data. The similarities between the nonstoichiometric $TiN_{0.55}$ and TiC are discussed.

I. INTRODUCTION

Many refractory materials (RM) which belong to the transition-metal compounds have found considerable interest because of their high superconducting transition temperatures T_c. In earlier work[1-3] we reported on the Raman scattering of the superconducting RM TiN, NbC, and ZrN. Good agreement between the phonon densities obtained from neutron scattering and the defect-induced first-order Raman spectra resembling the one-phonon density of states was observed in these cubic materials.[2,3]

It is well known that phonon anomalies[4-6] are closely linked to high transition temperatures T_c in the RM. Since the phonon density is influenced by phonon anomalies we thought it worthwhile to investigate the relations between the phonon density gained from defect- (vacancy-) induced Raman scattering and the superconductivity in the system TiN_x. Our results will be compared with yet unpublished phonon dispersion curves of TiN.[7] In addition, since samples with various Ti/N ratio are utilized for our study we wanted to give further evidence that we deal with first-order defect-induced Raman scattering.

II. SAMPLE PREPARATION AND EXPERIMENTAL

A. Sample preparation

1. Sample a

The TiN single crystal was prepared by chemical-vapor deposition from gas mixtures of $TiCl_4$, N_2, and H_2 on molybdenum tubes at temperatures of ~1600 °C. The nitrogen concentration was determined by the hot-extraction method. The size of the crystal is about $1 \times 1 \times 1$ mm^3.

2. Samples b, c, d

Polycrystalline titanium nitride was prepared from Ti 99.99% and N_2 99.99% by zone annealing. The nitrogen content was increased by annealing of 0.5-cm^3 samples of TiN_x in N_2 at 2700 °C for 65 h. The titanium content was determined by ignition of TiN_x to TiO_2, and the nitrogen content was taken as the difference between the total and the titanium content. The zone annealed specimens had the composition $TiN_{0.797}$ (sample *c*) and $TiN_{0.59}$ (sample *d*). After annealing in N_2, the composition was $TiN_{0.953}$ (sample *b*). In addition, the nitrogen concentration of the particular piece of sample *d* where the Raman experiments were performed was determined by the vacuum hot-extraction method as $x = 0.548$. In the following text the nitrogen concentration of samples *b*, *c*, and *d* is given by only two decimals. The data describing our samples are collected in Table I.

B. Experimental

The Raman scattering was measured with standard equipment,[1] consisting of an Argon laser operating with 1 W in the 488-nm line and a grating double monochromator with a photon counting detection system. The spectral resolution is about

TABLE I. Characterization of the TiN_x samples.

Sample	Color	x from chemical analysis	T_C[a] (K)	ΔT_C (K)	Lattice constant (Å)
a	Golden	$0.9950 \pm 5 \times 10^{-4}$	6.0 ± 0.1	0.02	$4.240 \pm 5 \times 10^{-4}$
b	Golden	$0.953 \pm 5 \times 10^{-3}$	1.7 ± 0.2[b]	0.3	$4.240 \pm 1 \times 10^{-3}$
c	Silver	$0.797 \pm 5 \times 10^{-3}$	<1.5[c]		$4.233 \pm 1 \times 10^{-3}$
d	Silver	$0.548 \pm 5 \times 10^{-3}$	<1.2[c]		$4.219 \pm 1 \times 10^{-3}$

[a]From resistance measurements.
[b]Temperature at which resistance has fallen to half the value at the onset of the drop at 2 K.
[c]No superconductivity was found above this temperature.

6 cm^{-1}; the absolute wave numbers are accurate by ± 3 cm^{-1}. The angle between the incident beam and the surface was about 20°, and the incident light was polarized in the plane of incidence. With this arrangement one works in the minimum of the reflected light intensity. The Raman scattering was measured on unpolished surfaces in order to exclude any perturbation by the polishing process. The temperature of the sample holder was 300 K. The spectra of sample *a* were measured with a dwell time of 100 sec at each point, the spectra of the samples *b* to *d* were measured continously with a ratemeter.

III. RESULTS

In Fig. 1, the Raman spectra of the samples *a*, *b*, *c*, and *d* up to 700 cm^{-1} are presented. The low-frequency scattering below 370 cm^{-1} is caused by acoustical phonons, the high-frequency scattering around 550 cm^{-1} is due to optical phonons.[1,2] As can be seen from Fig. 1, the scattering shifts continuously to higher frequencies the lower the nitrogen concentration of the TiN_x samples. This frequency shift is particularly pronounced in the range of acoustical phonons, where the lowest peak shifts from 200 cm^{-1} ($x_a = 0.995$) to 250 cm^{-1} ($x_d = 0.55$).

The position of the high-frequency peak of the almost stoichiometric sample with $x_a = 0.995$ [Fig. 1(a)] cannot be determined precisely because here two-phonon processes come into play (see Fig. 3). Therefore, a range of 520...550 cm^{-1} for the peak position is indicated in Fig. 1(a). Also, the second peak in Figs. 1(c) and 1(d) can only be located within a frequency range (330...360 cm^{-1}).

In Fig. 2(a), the frequency of the first peak of the acoustical range is plotted versus the deviation from stoichiometry. The main point of Fig. 2(a) is that for small deviations from stoichiometry $|1 - x_b| \sim 0.05$ the frequency of the first acoustical peak increases drastically $[(\bar{\nu}_b - \bar{\nu}_a)/\bar{\nu}_a \sim +18\%]$. For higher deviations, however, the peak frequency seems to reach the value of $\bar{\nu}_a \sim 250$ cm^{-1} asymptotically. Figure 2(b) contains the T_c values of our various TiN_x samples. In the same small deviation range $|1 - x_b| \sim 0.05$, in which the Raman peak frequency increases by 18%, T_c drops by more than 4 K (T_c of *a*: 6K; T_c of *b*: 1.7 K). Thus, the enormous drop in T_c parallels the drastic increase in the phonon frequency of the

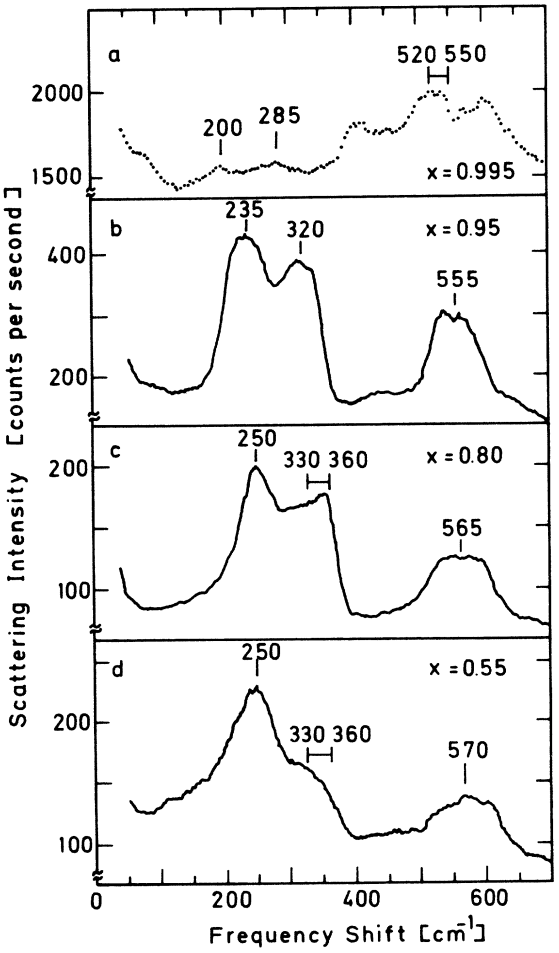

FIG. 1. Raman scattering intensities in counts per second of the TiN samples *a*, *b*, *c*, and *d* according to Table I.

first peak. It should be noted that the T_c value of the highly stoichiometric sample *a* is higher; the values for the nonstoichiometric samples *b* and *c* are lower than expected from Ref. 8.

Figure 3 shows the Raman spectra of the samples *a*, *b*, *c*, and *d* over a frequency range up to 1200 cm^{-1}. The spectrum of the almost stoichiometric sample [Fig. 3(a)] is dominated by strong peaks at ~400, ~600, ~800, ~1100, and probably also at about 500 cm^{-1}. These strong peaks of Fig. 3(a) are absent or weak compared to the two main scattering areas below 370 cm^{-1} (A: acoustical) and 520...580 cm^{-1} (O: optical) in the spectra of the nonstoichiometric samples *b*, *c*, and *d* [Figs. 3(b)–3(d)].

The main scattering areas of the samples *b*, *c*, and *d* (white in Fig. 3) are due to first-order Raman scattering.[1-3] As for Fig. 3(d), it seems as if the scattering of the acoustical range extends to almost the optical-frequency range, thus reducing the gap. The areas where the Raman scattering is strong in the almost stoichiometric sample are shaded throughout Fig. 3. These shaded scattering areas are caused by two-phonon scattering. Recently, we have attributed the structures at 800 and 1100 cm^{-1} to A + O and 2 O processes, respectively.[3] In addition, we now find according to Fig. 3(a) in the frequency range 370...700 cm^{-1}, where 2A processes may occur,[3] distinct peaks of the second-order spectrum.

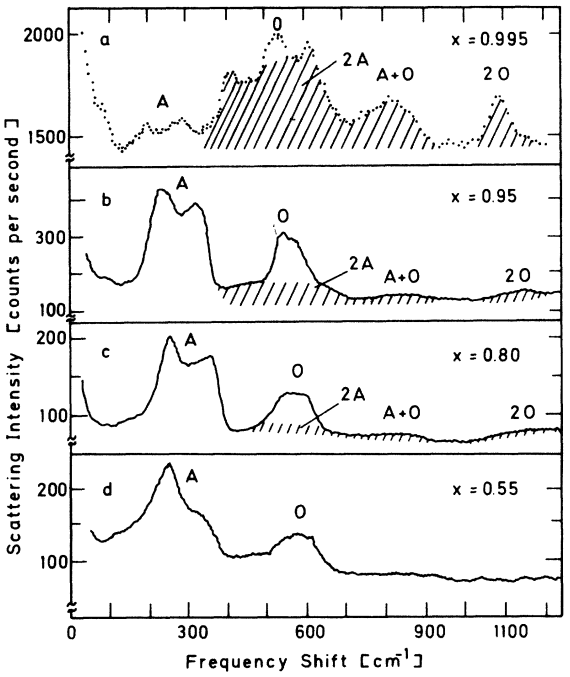

FIG. 3. First- and second-order Raman scattering intensities in counts per second of the TiN samples *a*, *b*, *c*, and *d* according to Table I.

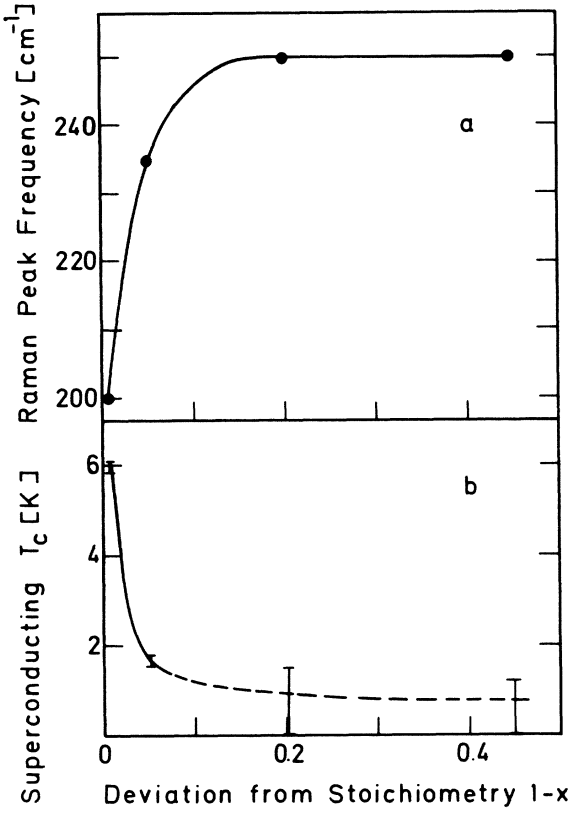

FIG. 2. Frequency of the first peak of the Raman scattering in the acoustical range of TiN_x (a) and superconducting critical temperature T_c (b) vs deviation from stoichiometry $1-x$.

It should be noted that according to Figs. 1 and 3 the intensity of the Raman scattering drops by one order of magnitude from sample *a* to sample *d*. This drastic decrease in intensity is due to the fact that the optical constants[9] which determine the penetration depth (~200 Å) change considerably from sample *a* to *d* and a resonance Raman effect in the almost stoichiometric samples[1,2] may occur. A consequence of the changing optical constants is the difference in color between the highly stoichiometric samples *a*, *b*, and the strongly nonstoichiometric samples *c* and *d* (see Table I).

IV. DISCUSSION

A. Raman spectra and phonon densities of states

The refractory materials (RM) such as TiN, TiC, ZrN, and NbC generally contain vacancies in both sublattices. This is true even for stoichiometric samples. In addition, there are the vacancies due to the deficiency of one component,

e.g., N. Because of these vacancies, defect-induced first-order Raman scattering in the cubic lattices of the RM is possible.[1-3] From this defect-induced first-order Raman scattering the perturbed projected phonon density of states can be obtained for the three Raman-active modes $A_{1g}(\Gamma_1)$, $E_g(\Gamma_{12})$, and $F_{2g}(\Gamma'_{25})$.[10] Our total Raman spectra of Figs. 1 and 3 contain the three Raman-active modes.

In the alkali halides the perturbed projected density of states differs from the density of the perfect crystal if the force constant between defect and first nearest neighbors is different from the force constant in the perfect crystal.[10] Assuming a similar situation in the RM one may conclude from the good agreement between the total Raman spectra and the phonon densities from neutron scattering in the RM[1-3] that the force constants are not too different in the environment of a vacancy (where the Raman-active vibration takes place) and in the total crystal (which is sampled by neutron scattering). It is questionable whether this model can be used for the RM which frequently contain large vacancy concentrations (> 10%).

B. First- and second-order scattering intensities

Previously,[1] we had found from the temperature dependence of the strong Raman bands of a TiN sample similar to sample b [Fig. 1(b)] that the scattering is of first order. In addition, we now obtain from Fig. 3 further proof for the first-order defect-induced scattering. The first-order scattering becomes more and more predominant the larger the deviation from stoichiometry, i.e., the defect concentration. This is analogous to the growing of the first-order Raman scattering intensity in NaCl with increasing impurity concentration (Ag^+) investigated by us earlier.[11]

In the NaCl : Ag^+ system for a defect concentration of a few percent we had observed contributions from defect pairs. If the vacancy concentration exceeds the order of 1%, the vacancies cannot be considered as isolated any more.

In connection with the spectrum of Fig. 3(a) we have already mentioned that the peaks between 370 and 700 cm^{-1} are caused by 2A processes, i.e., acoustical overtones and combinations. Thus, it is tempting to attribute the first five peaks of the spectrum 3a as follows: TA ~ 200, LA ~ 300, 2TA ~ 400, TA + LA ~ 500, 2LA ~ 600 cm^{-1}. The location of the TA and LA peaks is confirmed by phonon dispersion curves of TiN[7] which have come to our attention after completion of our experiments. The contributions from the various TA and LA phonon branches, in particular at the L point of the reciprocal lattice, are consistent with the location of the corresponding Raman peaks, while the contributions of the TO branches, again particularly at the L point, center at half the frequency of our 2O peak at 1100 cm^{-1}. Then, the A + O peak above 800 cm^{-1} must be attributed essentially to a LA + TO combination.

It is interesting to note that in the spectrum from optical overtones, according to Fig. 3(a), there is strong 2TO but no 2LO scattering. This is the same situation as in the alkali halides where the 2LO scattering is usually weak compared to the 2TO scattering.[12] In this connection we refer to the similarities between the second-order Raman spectra of RbF ($m_{Rb} \gg m_F$)[13] and TiN ($m_{Ti} \gg m_N$). Of course, for such a comparison the much stronger force constants in TiN, due to its partly covalent nature, must be accounted for.

As to the scattering intensities, one may assume that the scattering in the acoustical range is largely determined by vibrations of the heavy metal (Ti), while the scattering in the optical range is mainly determined by the lighter nonmetal (N) ion. According to Fig. 1 the ratio of the acoustical and optical scattering intensities increases with the defect concentration. One reason for this behavior is probably that in samples with high N deficiencies the optical scattering will be small because of a reduced number of vibrating N atoms. Moreover, in the nearly stoichiometric samples (a, b) the concentration of Ti vacancies (see Sec. II A) is possibly not negligible against the N vacancies from the N deficiency. The Ti vacancies with N atoms as first nearest neighbors may contribute to a relatively strong optical scattering in samples a and b.

C. Phonon anomalies; transition temperatures T_c

Since the phonon anomalies are closely linked to high T_c values, phonon anomalies in TiN are to be expected due to the high T_c values in stoichiometric material (sample a: 6 K, see Table I).

Of course, the phonon anomalies, which lead to minima in the acoustical branches of the phonon dispersion curves,[4-6] cannot be measured directly by Raman scattering. However, there is an indirect way: when the anomalies disappear in nonstoichiometric material, the frequencies in the particular acoustical phonon branch increase[14] and as a consequence, the density of the acoustical phonons shifts to higher frequencies. Recently, such a shift has been found for NbC[15] and NbN[16] from neutron scattering. Thus, a shift of the density distribution to higher frequency with increasing deviation from stoichiometry indicates anomalies.

TABLE II. Calculated values of $\langle\omega_{ac}^2\rangle^{1/2}$, $\langle\omega_{opt}^2\rangle^{1/2}$, $M\langle\omega^2\rangle$, and θ_∞ from the Raman spectra of the TiN samples *a* to *d* and TiC; θ_∞ from specific-heat data (Ref. 17); λ calculated after McMillan (Ref. 18).

Sample	T_C (K)	$\langle\omega_{ac}^2\rangle^{1/2}$ (cm^{-1})	$\langle\omega_{opt}^2\rangle^{1/2}$ (cm^{-1})	$M\langle\omega^2\rangle$ ($eV/Å^2$)	θ_∞ (K) This work	θ_∞ (K) Ref. 17	λ
$TiN_{0.995}$ (*a*)	6.0 ± 0.1	256	530 ± 15	26.1	487	485[a]	0.59
$TiN_{0.95}$ (*b*)	1.7 ± 0.1	273	561	29.5	518		0.45
$TiN_{0.80}$ (*c*)	<1.5	286	564	31.3	533		<0.44
$TiN_{0.55}$ (*d*)	<1.2	280 ± 20	573	31.0 ± 2.5	530 ± 20		<0.42
TiC	···	330	612	37.2	591	590	···

[a]For $TiN_{0.99}$ after Ref. 17.

Therefore, the large shift of the low-frequency part of the scattering due to acoustical phonons according to Figs. 1 and 2 (samples *a*–*d*: 200–250 cm^{-1}) and the good agreement between the total Raman spectra and the phonon densities[1-3] give strong evidence that there are phonon anomalies in the stoichiometric sample. This interpretation of the Raman results is fully justified by recent phonon-dispersion curve measurements of TiN.[7] In the acoustical branch of the dispersion curves of a $TiN_{0.98}$ sample the lowest frequency of the anomalies is located at 200 cm^{-1}. The phonon density around 200 cm^{-1} derived from the neutron data is in close agreement with the Raman data according to Figs. 1(a) ($TiN_{0.995}$) and 1(b) ($TiN_{0.95}$).

For a more detailed comparison of our various TiN_x samples the product of the mean-square frequencies $\langle\omega^2\rangle$ and the mass M was obtained from the Raman spectra considering the approximate relation used in Ref. 6 [Eq. (13)]

$$M\langle\omega^2\rangle = M_s\langle\omega_{ac}^2\rangle + M_r\langle\omega_{opt}^2\rangle;$$

$$(M_s = M_{Ti} + M_N;\ 1/M_r = 1/M_{Ti} + 1/M_N).$$

Consistent with previous work for the calculation of $\langle\omega^2\rangle$ the approximations α^2 = constant and $\langle\omega^2\rangle = \int\omega F\,d\omega / \int\omega^{-1}F\,d\omega$ have been used [6, 17]. The data for the various samples are collected in Table II. In two cases an insufficient separation of the first-order scattering results in a relatively large inaccuracy of $\langle\omega^2\rangle$. According to Table II, $\langle\omega_{ac}^2\rangle$ has its lowest value in the stoichiometric sample *a* with the highest T_c (6 K). With increasing N deficiency $\langle\omega_{ac}^2\rangle$ increases, while T_c decreases. The total decrease in $\langle\omega_{ac}^2\rangle$ between the nonstoichiometric samples *c*, *d*, and the almost stoichiometric sample *a* is about 20%.

Obviously, in TiN_x, the change of $\langle\omega_{ac}^2\rangle$ is stronger than in NbC_x,[15] where the change in $\langle\omega_{ac}^2\rangle$ between the nearly stoichiometric sample $NbC_{0.98}$ ($T_c \sim 11$ k) and the nonstoichiometric $NbC_{0.76}$ (no superconductivity was detected) is only about 10%.

It is interesting to note that in addition to the acoustical phonons the optical phonons also soften in direction to the stoichiometric sample *a* according to Table II, column 4. To our knowledge, the dependence of the optical phonons on the nonmetal deficiency has not been investigated systematically up to now.

$\langle\omega^2\rangle^{1/2}$ can be interpreted as a characteristic Debye temperature Θ_∞.[17] The calculated values of Θ_∞ are listed in the sixth column of Table II. It turns out that our value of Θ_∞ for stoichiometric TiN is in very good agreement with the value Θ_∞ obtained from specific-heat measurements[17] (see Table II).

Added to Table II are the values $\langle\omega^2\rangle$ and Θ_∞ from the Raman spectrum of TiC, Fig. 4(c). Also, for this system the agreement between Raman and specific-heat data is excellent. The last column of Table II contains the electron-phonon coupling

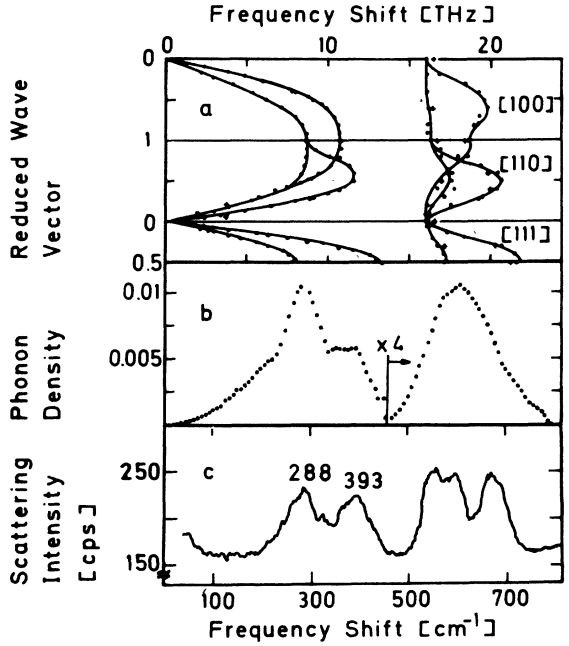

FIG. 4. Dispersion curves (a) and phonon density of states (b) of TiC after Ref. 20; (c) Raman scattering of TiC after Ref. 2.

constant λ which has been calculated from the McMillan[18] equation

$$T_c = \frac{\Theta}{1.45} \exp\left[-\left(\frac{1.04(1+\lambda)}{\lambda - \mu^*(1+0.62\lambda)}\right)\right], \quad (1)$$

with the Coulomb coupling constant μ^* taken as 0.13 (McMillan's average for the transition metals). Our calculated value of $\lambda = 0.59$ (sample *a*), see Table II, last column, compares well with the λ value of 0.54 given by Weber.[6] It must be added, though, that Weber used a different Debye temperature and a TiN which was less stoichiometric ($T_c = 5.49$ K) than our sample *a* ($T_c = 6$ K). Our λ values, according to Table II, decrease from 0.59 in the almost stoichiometric sample, to lower values in the nonstoichiometric samples as a consequence of the lower T_c values. From sample *a* to sample *b*, λ decreases by 30%, whereas $M\langle\omega^2\rangle$ increases by roughly 10%. Therefore, it seems that in TiN λ is not inversely proportional to $M\langle\omega^2\rangle$.[18] The same situation was found for other RM.[6,19]

D. TiN and TiC

Whereas two of our TiN_x samples *a* ($x_a = 0.995$) and *b* ($x_b = 0.95$) are superconducting, the highly nonstochiometric samples *c* ($x_c = 0.80$) and *d* ($x_d = 0.55$) are nonsuperconducting above 1.5 K and 1.2 K, respectively. According to the results of Fig. 2, the anomalies have largely disappeared in these highly nonstoichiometric samples. Both superconductivity and phonon anomalies are linked to the number of valence electrons and fade away if the number of valence electrons drops to eight. Obviously, in $TiN_{0.55}$ the number of valence electrons has decreased sufficiently. If so, one may expect that the phonon density of $TiN_{0.55}$ behaves similar to the phonon density of TiC with eight valence electrons.

In Fig. 4, the phonon dispersion curves [Fig. 4(a)] along with the phonon densities [Fig. 4(b)] obtained from neutron scattering[20] are presented. Figure 4(c) shows the Raman spectrum of TiC investigated by us earlier.[2] Incidentally, the Raman spectrum reveals peaks in the phonon density which are to be expected from the dispersion curves, but which are lacking in the phonon density from neutron scattering due to insufficient resolution. This is particularly true of the density of the optical phonons.

From a comparison of Figs. 1 and Fig. 4(c), one recognizes that indeed the acoustical phonon density of the TiN sample with the largest N deficiency (*d*: $1 - x = 0.45$) is shifted in direction to the phonon density of TiC with eight valence electrons. Obviously, the situation in TiN is similar to the situation in NbC, where samples with large carbon deficiencies ($NbC_{0.76}$)[14] are nonsuperconducting and show no phonon anomalies.

In the optical range of a hypothetical TiC calculated from $TiN_{0.55}$, after taking into account the lower mass of the carbon instead of nitrogen, the calculated optical frequency is higher than in TiC as expected from the corresponding situation in the systems $NbC_{0.76}$ (high TO frequency) and ZrC (low TO frequency).[5]

V. CONCLUSION

In TiN_x, as in alkali halides with impurities, first-order Raman scattering resembling the one-phonon density of states is possible because in cubic TiN_x with N vacancies as in alkali halides containing impurities the translational and the inversion symmetry are broken by the defects.

We have shown that in the refractory material TiN_x first-order Raman peak frequencies in the acoustical range and superconducting transition temperatures T_c are closely linked together and valuable information on the phonon densities, e.g., phonon anomalies, can be obtained from Raman studies.

TiN is no exception. We have already found defect-induced Raman scattering for the superconducting cubic refractory materials ZrN and NbC.[2,3] It is interesting to note that also in the cubic antiferromagnet GdS, which belongs like the refractory materials to the transition-metal compounds, defect-induced first-order Raman scattering has been discovered.[21] Thus, it seems that Raman spectroscopy is suitable for investigations of a wide class of cubic metallic materials.

ACKNOWLEDGMENTS

We are grateful to Professors W. Gläser and H. Bilz for stimulating discussions, to the authors of Ref. 7 for making the neutron dispersion curves available to us prior to publication; to Dr. H. Schneider, Kernforschungszentrum Karlsruhe, for the chemical analysis of sample *d*; and to Dr. P. Berberich, Technische Universität München for performing a T_c measurement.

†Work supported by the Deutsche Forschungsgemeinschaft.

[1]W. Spengler, R. Kaiser, and H. Bilz, Solid State Commun. 17, 19 (1975).

[2]W. Spengler, R. Kaiser, and H. Bilz, *Proceedings of the Third International Conference on Light Scattering in Solids, Campinas, 1975*, in *Light Scattering in Solids*, edited by M. Balkanski *et al*. (Flammarion,

Paris, 1976), p. 81.
[3]W. Spengler and R. Kaiser, Solid State Commun. 18, 881 (1976).
[4]H. G. Smith and W. Gläser, Phys. Rev. Lett. 25, 1611 (1970).
[5]W. Weber, Phys. Rev. B 8, 5082 (1973); W. Weber, H. Bilz, and U. Schröder, Phys. Rev. Lett. 28, 600 (1972).
[6]W. Weber, Phys. Rev. B 8, 5093 (1973).
[7]W. Kress, P. Roedhammer, H. Bilz, W. D. Teuchert, and A. N. Christensen, Phys. Rev. B 17, 111 (1978).
[8]L. E. Toth, *Transition Metal Carbides and Nitrides* (Academic, New York, 1971), p. 220.
[9]H. Knosp and H. Goretzki, Z. Metallkd. 60, 587 (1969).
[10]G. Benedek and G. F. Nardelli, Phys. Rev. 154, 872 (1967).
[11]W. Möller and R. Kaiser, Z. Naturforsch. A 25, 1024 (1970); W. Möller, R. Kaiser, and H. Bilz, Phys. Lett. A 32, 171 (1970).
[12]R. Haberkorn, M. Buchanan, and H. Bilz, Solid State Commun. 12, 681 (1973).
[13]R. R. Hayes and K. H. Rieder, Phys. Rev. B 8, 5972 (1973).
[14]H. G. Smith and W. Gläser, *Proceedings of the International Conference on Phonons, Rennes, 1971*, edited by M. A. Nusimovici (Flammarion, Paris, 1971), p. 145.
[15](a) F. Gompf, Prog. Rep. Teilinstit. Nukl. Festkörperphys. Ges. Kernforsch. Karlsruhe KFK 2357, 8 (1976); (b) F. Gompf, L. Pintschovius, W. Reichardt, and G. Scheerer, *Proceedings of the Conference on Neutron Scattering*, edited by R. M. Moon (Natl. Tech. Info. Ser. (U.S. Dept. of Commerce, Springfield, Va., 1976), Vol. 1, p. 129.
[16]F. Gompf, W. Reichardt, and A. N. Christensen, Prog. Rep. Teilinstit. Nukl. Festkörperphys., Ges. Kernforsch. Karlsruhe KFK 2357, 11 (1976).
[17]P. Roedhammer, W. Weber, E. Gmelin, and K. H. Rieder, J. Chem. Phys. 64, 581 (1976); P. Roedhammer, E. Gmelin, W. Weber, and J. P. Remeika, Phys. Rev. B 15, 711 (1977).
[18]W. L. McMillan, Phys. Rev. 167, 331 (1968).
[19]P. B. Allen and M. L. Cohen, Phys. Rev. Lett. 29, 1593 (1972).
[20]L. Pintschovius and W. Reichardt, Prog. Rep. Teilinstit. Nukl. Festkörperphys., Ges. Kernforsch. Karlsruhe KFK 2357, 1 (1976); Ref. 15(b), Vol. 1, p. 129.
[21]E. Anastassakis, H. Bilz, M. Cardona, P. Grünberg, and W. Zinn, *Proceedings of the Third International Conference on Light Scattering in Solids, Campinas, 1975*, in *Light Scattering in Solids*, edited by M. Balkanski *et al*. (Flammarion, Paris, 1976), p. 367.